EXPERIMENTAL STUDY OF Au AND Ag PHASES DURING CRYSTALLIZATION OF Cu–Fe SULFIDE MELT

Tatyana A. Kravchenko and Elena N. Nigmatulina
Institute of Mineralogy and Petrography, Siberian Branch RAS, Novosibrsk, tanyuk@uiggm.nsc.ru

Species of trace Au and Ag (1 wt.%) in crystallized products of the central part melts of the Cu-Fe-S system have been studied. It has been established that gold of high fineness (80–82 wt.%) and silver (98–99 wt.%) associated with cubic (pc) haycockite $Cu_4Fe_5S_8$ solid solution, bornite Cu_5FeS_4 and pyrrhotite $Fe_{1-x}S$ crystallize from melts containing 47 at.% S, Cu/Fe = 0.93–0.63. Gold of high fineness (84–96 wt.%) and sulfides of the Me_2S type, where Me is up to, at.%: 48 Ag, 23 Au, 18 Cu, 2 Fe, associated with tetragonal chalcopyrite solid solution $Cu_{1-x}Fe_{1+x}S_2$, cubanite $CuFe_2S_3$, talnakhite $Cu_9Fe_8S_{16}$, pyrite FS_2, bornite, and pyrrhotite crystallize from melts of the following composition: 50 at.% S, Cu/Fe = 1–0.43 and 47 at.% S, Cu/Fe = 1.12. It is concluded that the Ag-Au sulfides are formed at temperature higher than 600°C and are resulted from a presence of free sulfur after crystallization of high-temperature cubic (fcc) chalcopyrite solid solution (iss). The relations of the Au-Ag phases and Cu-Fe sulfides in the products of joint crystallization from melts are determined by accumulation of Au-Ag phases during crystallization of iss and fine scattering of Ag as Ag-bearing sulfides are formed.
1 table, 8 figures, 13 references.
Keywords: gold, silver, Cu-Fe-S system.

Introduction

Au and Ag are elements identified in all types of deposits, where they are mainly associated with sulfide ore. Despite numerous studies, the problems concerning mechanism of accumulation and species of these elements in the ore-forming sulfides are unsolved. The magmatic deposits are the least studied. Therefore, the experimental study of Au and Ag behavior during melt crystallization together with sulfides of the Cu-Fe-S system, pyrite FS_2, chalcopyrite $CuFeS_2$, and pyrrhotite $Fe_{1-x}S$, which are major carriers of Au and Ag in sulfide ores is topical. At the same time, the study of crystallization of sulfide melt as probable mechanism of initial gold and silver accumulation is interesting to understand the conditions of formation of Au-Ag deposits of variable genesis.

Many scientists studied the Cu-Fe-S system. The experimental data of phase relations involving pyrite, chalcopyrite, and pyrrhotite (Yund & Kullerud, 1966; Cabri, 1973; Sugaki *et al.*, 1975; Vaughan & Craig, 1978, Tsujmura & Kitakaze, 2004) in general are consistent with the results of study of these minerals (Genkin *et al.*, 1981) in the Noril'sk Cu-Ni magmatic deposit, where up to 150 ppm Ag were detected in chalcopyrite and average 13 ppm Au, in pyrrhotite (Sluzhenikin & Mokhov, 2002). The Au-Ag solid solutions and acanthite Ag_2S are the most abundant proper mineral phases of Au and Ag. These compounds are attributed to the Ag-Au-S system that was completely studied by Barton (1980), who had revealed phase relations, temperatures of phase transitions, and melt temperatures of sulfides. However, available experimental data are insufficient to interpret the conditions of formation of natural sulfide assemblages, where Au and Ag are traces.

The aim of this study is to investigate the behavior of Au and Ag admixture during crystallization from melt together with sulfides of the Cu-Fe-S system, chalcopyrite, pyrite, and pyrrhotite. The features of chemical composition of synthesized phases are not discussed. The focus is on determination of Au and Ag phases depending on composition of synthesized assemblages of Cu-Fe sulfides.

Experimental

The Cu-Fe-S system was used as model macrosystem, where Au and Ag are as microconstituents (traces). In this case, the species of traces are suggested to be determined by physicochemical conditions of crystallization of equilibrium assemblages of Cu-Fe sulfides (macrocomponents). According to

this, the regime of synthesis of phase assemblages of macrosystem was established by melt cooling. Au and Ag (1 wt.%) were introduced in the synthesized samples of macrosystem and regime of synthesis corresponded to that of Cu-Fe sulfide assemblages. Amount of introduced traces is caused by difficult detection of contents below 1 wt.% by microscope and electron microprobe.

The plot of phase relations in the central Cu-Fe-S system constructed by Cabri (1973) was used as basis to select initial melt compositions. This plot is consistent with results of most experimental data on the Cu-Fe-S system and probable high- and low-temperature phase assemblages containing chalcopyrite, pyrite, and pyrrhotite are shown in it. In Fig. 1, the chalcopyrite solid solution field (iss) corresponds to the high-temperature cubic solid solution with face centered (fcc) lattice. It was experimentally established at 800–300°C and named by Merwin & Lombard (1937) as intermediate iss and Yund & Kullerud (1966) called this as chalcopyrite solid solution. Cubanite $CuFe_2S_3$, talnakhite $Cu_9Fe_8S_{16}$, mooihoekite $Cu_9Fe_9S_{16}$, and haycockite $Cu_4Fe_5S_8$ are attributed to the composition field of this solid solution. At the same time, these minerals compose Cu-rich ores of the Noril'sk Cu-Ni deposits. The iss field decreases as temperature drops and its lower boundary corresponds to the 47 at. % S section. The initial compositions of the synthesized samples involving the field of probable phase assemblages of chalcopyrite with pyrite, pyrrhotite, and aforementioned iss crystallized products are shown as black circles 1–9 in Fig. 1. The samples of composition ranging from chalcopyrite to iss with maximum Fe (Cu/Fe 1–0.43) were synthesized along section 50 at.% S and those of composition varying from iss with maximum Cu to iss with maximum Fe (Cu/Fe 1.12–0.63) were synthesized at 300°C along section 47 at.% S. The samples of the Cu-Fe-S system were synthesized from elements: carbonyl iron A-2 (granules), copper B3, and ultrapure sulfur additionally dehydrated by melting in vacuum superfine (pieces). Au and Ag were introduced in the Cu-Fe-S synthesized samples as pieces of Au-Ag alloy (by 50 wt.%). The samples weighted 110–120 mg. All samples were synthesized in vacuum quartz vials by heating up to 1100°C, storage at 1100°C for 12 h, cooling down to 850°C with step 50°C/h, storage at 850°C for 72 h, cooling down to 300°C with step 50°C/h, and cooling down to room temperature at switched off furnace. The rate of melt cooling was selected through experiment for the synthesis of all Cu-Fe-S samples by the same regime and following estimation of gold and silver behavior depending on composition of synthesized assemblages of Cu-Fe sulfides. The sample were cooled from 300°C with

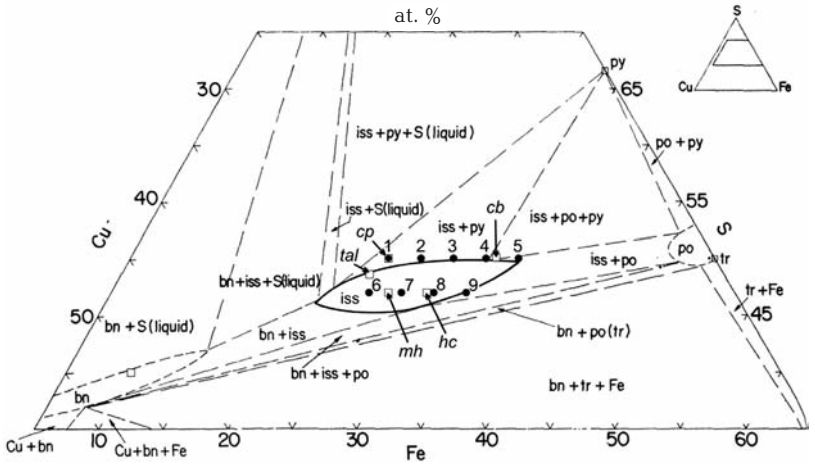

Fig. 1. Phase relations in the central part of the Cu-Fe-S system at 600°C (Cabri, 1973). Squares denote stoichiometric compositions of chalcopyrite $CuFeS_2$ (cp), talnakhite $Cu_9Fe_8S_{16}$ (tal), mooihoekite $Cu_9Fe_9S_{16}$ (mh), haycockite Cu_4Fe5S_8 (hc), bornite Cu_5FeS_4 (bn), cubanite $CuFe_2S_3$ (cb), troilite FeS (tr), and pyrite FeS_2 (py); po – pyrrhotite $Fe_{1-x}S$. Filled circles 1-9 denote initial composition of synthesized samples.

switched off furnace to obtain low-temperature crystallized products of iss rather than hardening.

After synthesis, the crystallized products were studied with optical microscope and X-ray diffraction. Polished sections were prepared from half of each sample (cut through the centre from the top down). The chemical composition of phases and distribution of traces in the sample bodies were detected by a Camebax-Micro electron microprobe according to the RMA-96 universal program (Lavrent'ev & Usova, 1991). The following analytic lines were used: Fe K_α, Cu K_α, S K_α, Ag L_α, Au M_α. In this set, lines are not superimposed. A probable interference of Cu K_{β_1} and Ag L_α in the third order reflection was taken into account by the PLATIN20DEL subroutine built-in RMA-96 program. This subroutine is matrix of delta coefficients taking into account the cross-effect of elements. The following standards were used: $CuFeS_2$, Au, and Ag. Operating conditions are 20 kV, 40 nA, counting time 10 s, and beam diameter 2–3 microns. All components were detected with accuracy of 2 relative percents. The detection limit calculated according to the 2δ test at 99% significance level is as follows, wt.%: 0.04 Cu, 0.03 Fe, 0.01 S, 0.05 Au, 0.04 Ag. BSE images of interrelated synthesized phases were made with JSM 5300 and JSM 6380 LA scanning electron microscopes in Institute of Geology of ore Deposits, Petrography, Mineralogy, and Geochemistry, Russian Academy of Sciences, Moscow, analysts S.F. Sluzhenikin and A.V. Mokhov (Kravchenko *et al.*, 2005; Kravchenko & Nigmatulina, 2007).

Results

The results of investigation of crystallized products of melts containing by 1 wt. % Au and Ag in the central Cu-Fe-S system are given in Table and in Fig. 2. The Cu-Fe-S phases are called master phases, whereas gold and silver phases, impurity phases. In this case, names of mineral analogues are applied to denote the master phases. The Au-Ag alloys of high fineness (> 75 wt.% Au) and silver (98–99 wt.% Ag) are shown as chemical symbols Au and Ag. Other phases containing Au and Ag are denoted as generalized chemical formulas taking into account element whose content is not less than 5 at.%.

The sample 1 matrix is composed of stoichiometric chalcopyrite. Bornite and pyrite occur along margins mainly on the upper surface of ingot (Fig. 2a). The impurity phases crystallize as fine drops and veinlets in the whole body of the sample that hampers their determination. Optical microscopy of great magnification indicates that these phases are characterized by different reflection and are located at the grain boundaries of master phases, in pores and fractures, and on the surface of the sample. The composition of the largest and brightest grains corresponds to gold of high fineness with minor Cu and Fe (Fig. 2b). The grains with less reflection were examined only in the margins of the sample. These are sulfides $(Ag,Au,Cu)_2S$ (Fig. 2c). Variable Ag content (0–0.8 wt.%) was detected in chalcopyrite and bornite both in various grains and within the single grain.

Sample 2 is predominantly composed of chalcopyrite (Fig. 3a). Cubanite $CuFe_2S_3$ as exsolution texture was identified in chalcopyrite being studied at high magnification (Fig. 3d). Like sample 1, gold of high fineness is located between chalcopyrite grains (Fig. 3c). The largest grains of impurity phases occur on the sample surface and are sulfide $(Ag,Cu)_2S$ and Au-Ag alloy (Fig. 3, 3b). In addition to gold, fine white grains with lesser reflection are observed (Figs. 3c, 3d). Analyses of master phases containing such phases are given in Table as (cp + cb)*.

In samples 3 and 4, master phases are chalcopyrite, cubanite, and pyrite (Fig. 4a) and in sample 5, additional pyrrhotite (Fig. 5a). Insignificant bornite occurs on the surface of these samples (Figs. 4c, 5a, 5d). Like sample 5, chalcopyrite and cubanite form exsolution texture, which can be observed only at high magnification (Figs. 4b, 5c). The composition of Au-Ag phases and their relations to Cu-Fe sulfides are similar to those described in sample 1 (Figs. 4b, 4c, 5b, 5d, 5e).

In sample 6, three phase occur as exsolution texture. In composition, these are chalcopyrite, talnakhite, and bornite (Fig. 6a). The grain of Au-Ag alloy whose composition is given in Table is shown in Fig. 6b. Other Au- and Ag-bearing phases were detected

Table 1. **Crystallized products of the Cu-Fe-S melts containing by 1 wt.% Ag and Au**

№	Initial composition: S; Cu; Fe, at.% Cu/Fe	Synthesized phases	Composition: at.%, wt.% Ag	Au	Cu	Fe	S	Total, wt.%
1	50; 25; 25	cp	0.03	0.00	25.03	24.48	50.47	
	1		0.06	0.00	34.48	29.64	35.08	99.26
		py	0.00	0.00	0.087	33.08	66.83	
			0.00	0.00	0.138	46.40	53.80	100.34
		bn	0.39	0.00	49.74	7.86	42.02	
			0.85	0.00	63.77	8.86	27.17	100.65
		Au	7.22	80.72	7.45	4.61	0.00	
			4.50	91.71	2.73	1.49	0.00	100.43
		$(Ag,Au,Cu)_2S$	40.16	12.99	10.20	1.61	35.05	
			50.53	29.84	7.56	1.05	13.11	102.09
		The same	29.45	22.74	5.81	2.41	39.58	
			34.35	48.44	3.99	1.46	13.73	101.97
2	50; 22.5; 27.5	cp	0.09	0.00	23.61	26.22	50.07	
	0.82		0.21	0.00	32.61	31.83	34.89	99.54
		cb	0.14	0.00	18.66	30.38	50.81	
			0.33	0.00	25.99	37.26	35.76	99.34
		Au	4.61	90.46	1.97	2.96	0.00	
			2.68	95.88	0.68	0.89	0.00	100.12
		$(Ag,Cu)_2S$	47.71	0.00	18.24	0.67	32.78	
			66.17	0.00	16.09	0.50	14.13	99.89
		(cp+cb)*	19.83	0.00	16.96	21.20	42.01	
			37.31	0.00	18.80	20.65	23.50	100.26
3	50; 20; 30	cp	0.24	0.00	22.64	27.21	49.92	
	0.67		0.56	0.00	32.78	31.03	34.53	98.90
		cb	0.11	0.00	16.91	32.53	50.45	
			0.26	0.00	23.37	39.52	35.19	98.34
		py	0.00	0.00	0.17	33.41	66.41	
			0.00	0.00	0.27	46.26	52.78	99.31
		bn	0.67	0.00	50.27	8.64	40.42	
			1.43	0.00	62.80	9.48	25.48	99.19
		Au	23.44	71.77	3.11	1.03	0.654	
			14.98	83.77	1.17	0.34	0.124	100.39
		$(Cu,Ag)_3S_2$	18.63	0.84	38.64	0.67	41.22	
			33.54	2.78	40.98	0.62	22.05	99.97
4	50; 17.5; 32.5	cp	0.17	0.00	21.07	28.53	50.23	
	0.54		0.41	0.00	29.03	34.56	34.92	98.92
		cb	0.09	0.00	17.74	31.01	51.16	
			0.28	0.00	25.25	38.00	35.80	99.53
		py	0.00	0.00	0.04	33.33	66.63	
			0.00	0.00	0.06	46.13	52.94	99.14
		bn	0.23	0.00	51.90	7.54	40.33	
			0.49	0.00	64.83	8.27	25.41	99.00
		Au	17.08	78.48	2.81	0.95	0.68	
			10.50	87.84	1.01	0.30	0.12	99.97
		$(Ag,Au,Cu)_3S_2$	27.02	13.09	14.73	1.13	44.03	
			36.72	32.58	11.81	0.78	17.94	99.83
5	50; 15; 35	cp	0.27	0.00	19.54	29.93	50.26	
	0.43		0.63	0.00	27.02	36.37	35.06	99.08

Table 1. **Continuation**

		cb	0.33	0.00	17. 68	31.49	50.50	
			0.77	0.00	24.54	38.40	35.35	99.06
		po	0.00	0.00	0.42	46.05	53,53	
			0.00	0.00	0.62	59.20	39.51	99.33
		py	0.00	0.00	0.12	33.21	66.67	
			0.00	0.00	0.19	46.14	53.17	99.50
		bn	0.44	0.00	52.53	7.14	39.88	
			0.92	0.00	65.54	7.84	25.10	99.40
		Au	6.23	84.55	3.88	4.43	0.92	
			3.72	92.31	1.37	1.37	0.16	98.93
		$(Ag,Au,Cu)_2S$	30.72	13.65	16.17	1.60	37.87	
			40.64	32.97	12.60	1.09	14.89	102.19
6	47; 28; 25	cp	0.00	0.00	25.43	24.71	49.86	
	1.12		0.00	0.00	34.86	29.76	34.48	99.10
		tal	0.00	0.00	27.04	24.12	48.84	
			0.00	0.00	36.68	28.75	33.42	98.85
		bn	0.06	0.00	48.76	11.26	39.92	
			0.12	0.00	62.35	12.66	25.76	100.89
		Au	10.44	82.18	3.79	2.63	0.96	
			6.31	90.74	1.35	0.82	0.18	99.40
		(bn + cp)*	10.33	0.00	34.87	16.65	38.15	
			20.19	0.00	40.13	16.84	22.15	99.31
		(cp + tal)*	13.77	0.00	24.74	21.16	40.13	
			26.24	0.00	28.29	21.77	23.27	99.58
7	47; 25.5; 27.5	hk	0.00	0.00	24.08	28.17	47.76	
	0.93		0.00	0.00	32.81	33.74	32.84	99.39
		bn	0.00	0.00	52.81	9.14	48.05	
			0.00	0.00	67.32	10.24	24.47	102.03
		Au	25.36	66.48	7.39	0.17	0.60	
			16.75	80.15	2.87	0.06	0.12	99.95
		Ag	97.86	0.00	1.44	0.56	0.14	
			97.90	0.00	0.84	0.29	0.04	99.07
8	47; 23; 30	hk	0.00	0.00	23.29	29.19	47.52	
	0.77		0.00	0.00	31.73	34.96	32.68	99.36
		bn	0.00	0.00	49.20	10.85	39.95	
			0.00	0.00	62.87	12.18	25.75	100.80
		Au	19.82	68.39	10.02	1.27	0.49	
			13.12	82.36	3.90	0.44	0.10	99.92
		Ag	98.32	0.00	0.89	0.57	0.22	
			99.52	0.00	0.53	0.30	0.07	100.42
9	47; 20.5; 32.5	hk	0.00	0.00	22.56	30.12	47.32	
	0.63		0.00	0.00	30.75	36.09	32.55	99.39
		bn	0.00	0.00	49.20	10.85	39.95	
			0.00	0.00	62.87	12.18	22.75	100.80
		po	0.00	0.00	1.65	47.85	50.49	
			0.00	0.00	2.37	60.46	36.62	99.46
		Au	20.34	66.92	11.57	1.00	0.17	
			13.54	81.28	4.54	0.35	0.03	99.74
		Ag	98.01	0.00	1.01	0.69	0.29	
			99.10	0.00	0.60	0.36	0.09	100.15

Notes: (cp) chalcopyrite $CuFeS_2$, (py) pyrite FeS_2, (bn) bornite Cu_5FeS_4, (cb) cubanite $CuFe_2S_3$, (tal) talnakhite $Cu_9Fe_8S_{16}$, (hc) haycockite $Cu_4Fe_5S_8$, (po) pyrrhotite ($Fe_{1-x}S$), (*) Cu-Fe sulfides with fine disseminated Ag-bearing phases

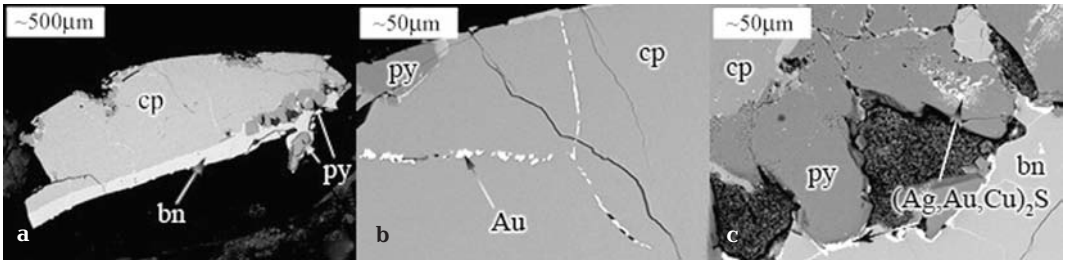

Fig. 2. Sample 1: a — common view of the sample with chalcopyrite (cp), bornite (bn), and pyrite; b — gold between grains of chalcopyrite; c — Ag-Au-Cu sulfides in pyrite and between grains of pyrite and bornite.

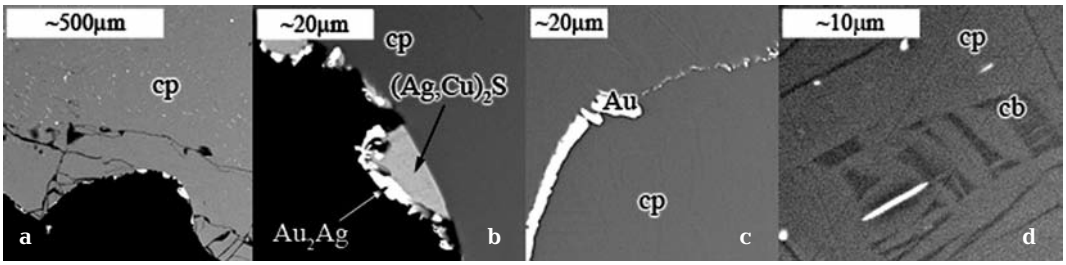

Fig. 3. Sample 2. Au-Ag phases (white) associated with chalcopyrite (cp) and cubanite (cb): a, b — chalcopyrite matrix, $(Ag,Cu)_2S$ sulfides and Au-Ag alloys on the sample surface; c — gold of high fineness between grains of chalcopyrite; d — chalcopyrite-cubanite matrix.

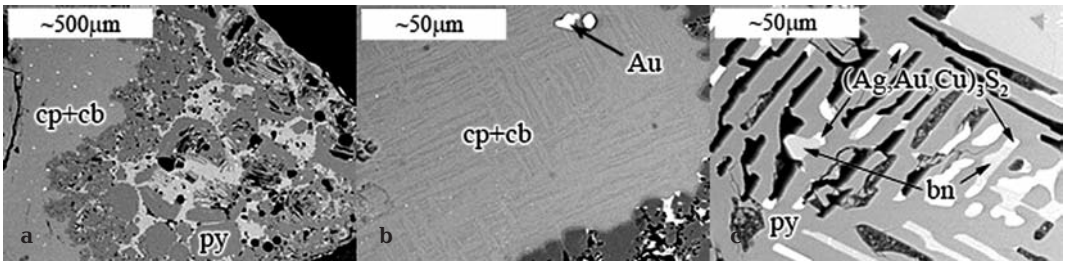

Fig. 4. Sample 4: a — Au-Ag phases (white) associated with chalcopyrite (cp), cubanite (cb), pyrite (py), and bornite (bn); b — gold in chalcopyrite-cubanite matrix; c — Ag-Au-Cu sulfides associated with pyrite and bornite near sample surface.

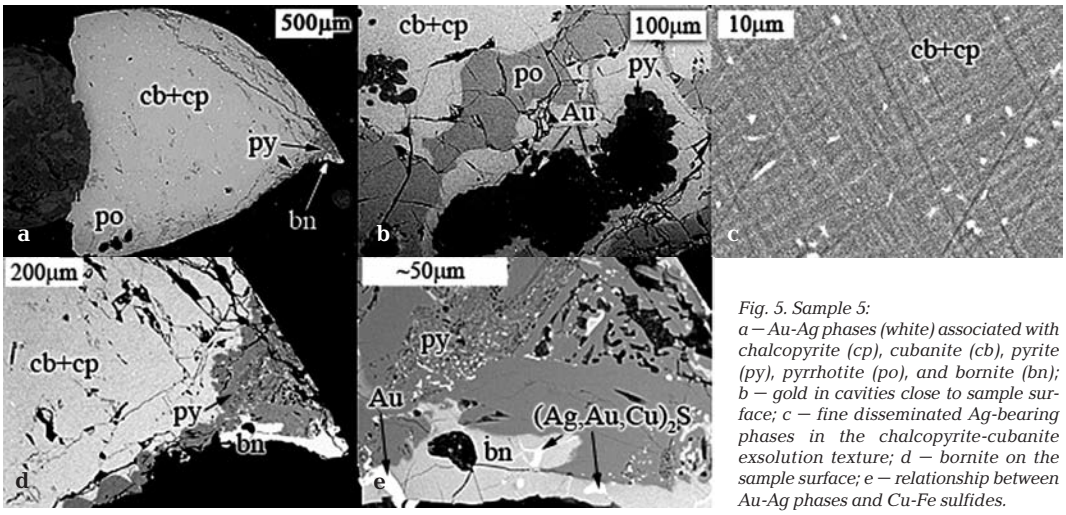

Fig. 5. Sample 5:
a — Au-Ag phases (white) associated with chalcopyrite (cp), cubanite (cb), pyrite (py), pyrrhotite (po), and bornite (bn); b — gold in cavities close to sample surface; c — fine disseminated Ag-bearing phases in the chalcopyrite-cubanite exsolution texture; d — bornite on the sample surface; e — relationship between Au-Ag phases and Cu-Fe sulfides.

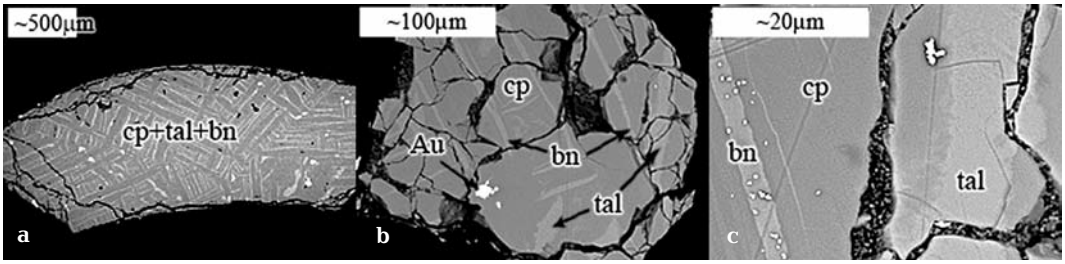

Fig. 6. Sample 6: a — Au-Ag phases (white) associated with chalcopyrite (cp), talnakhite (tal), and bornite (bn); b — gold close near sample surface; c — fine disseminated Ag-beraing phases in chalcopyrite and talnakhite.

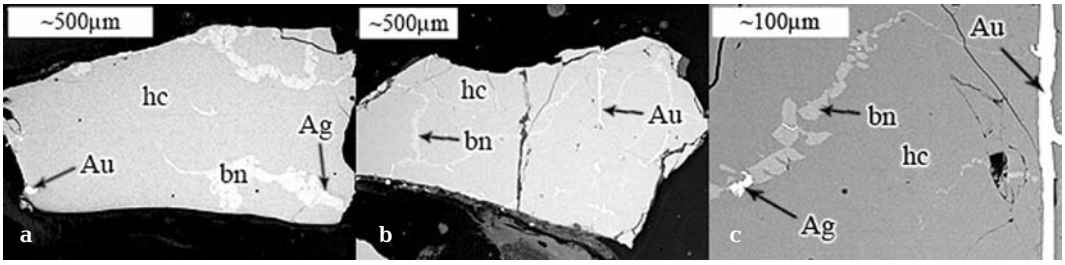

Fig. 7. Gold and silver (white) associated with haycockite (hc) and bornite (bn): a — sample 7; c, d — sample 8.

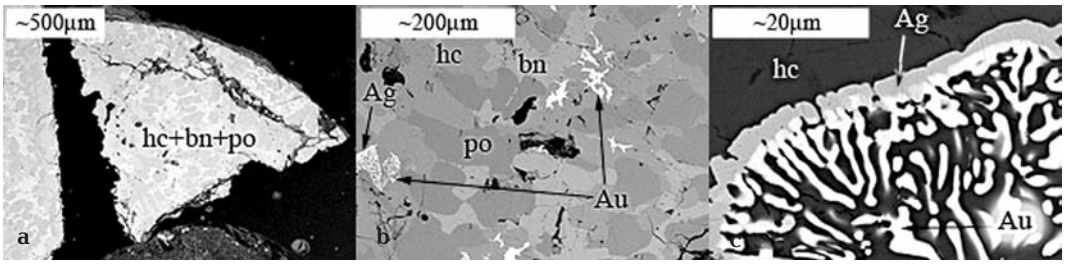

Fig. 8. Sample 9: a — gold and silver (white) associated with haycockite (hc), bornite (bn), and pyrrhotite (po); b — gold and silver between grains of pyrrhotite, haycockite, and bornite; c — Au-Ag zoned grain.

with scanning electron microscope (Fig. 6c). Like aforementioned samples, maximum content of impurities was identified at the grain boundaries of master phases (Table, bn + cp*, cp + tal*).

Samples 7 and 8 consist of bornite, phase of composition close to haycockite, and gold and silver of high fineness (Fig. 7). In sample 9, pyrrhotite occurs along with bornite and haycockite (Fig. 8a). In contrast to above described samples, Au-Ag alloys of samples 7—9 contain higher Ag, and silver crystallize together with them rather than Ag and Au sulfides (Figs. 7, 8). Some Au-Ag grains are zoned (Figs. 8b, 8c). Like samples 1—6, impurity phases occur at the grain boundaries of master phases and on the sample surface.

Thus, the assemblages of Cu-Fe sulfides stable at room temperature and corresponding in composition to initial composition of melts shown in Fig 1 were synthesized: sample 1 — chalcopyrite + bornite + pyrite; samples 2—4 — chalcopyrite + cubanite + pyrite; sample 5 — chalcopyrite + cubanite + pyrite + pyrrhotite; sample 6 — chalcopyrite + talnakhite + bornite; samples 7, 8 — haycockite + bornite; sample 9 — haycockite + bornite + pyrrhotite. The results obtained are consistent with experimental study (Cabri, 1973). At room temperature, chalcopyrite or chalcopyrite with cubanite along section 50 at.% and talnakhite or haycockite along section 47 at.% were synthesized instead of iss (Fig. 1).

Proper phases of Au and Ag are established in all synthesized phases. Gold of high fineness (80—82 wt.%) and silver (98—99 wt.%) crystallize from melts contain-

ing 47 at.% S, Cu/Fe = 0.93–0.63 (samples 7–9). Gold of high fineness (84–96 wt.%) and Ag-Au sulfides of the Me_2S or Me_2S_3 type where Me is Ag (up to 48 at.%), Au (up to 23 at.%), Cu (up to 18 at.%), and Fe (up to 2 at.%) crystallize from the melts containing 50 at.% S, Cu/Fe = 1.0–0.43 and 47 at.%, Cu/Fe = 1.12 (samples 1–6). Extremely fine grains of Ag-Au sulfides prevent exact determination of composition of these compounds. Variable Ag content (0–0.8 wt.%) was detected by electron microprobe in master phases of samples 1–6. In electron microscope, fine disseminated Ag-bearing phases are observed in the master phases. The bulk chemical composition of master phases and impurity phases corresponds to the compositions of mixtures of chalcopyrite with cubanite, bornite, and talnakhite containing up to 37 wt.% Ag (Table, cp + cb*, cp + bn*, cp + tal*).

The fine grains distributed through all samples are characteristic of all Au-Ag phases. In the case, they are predominantly arranged at the boundaries of Cu-Fe sulfide grains, in pores, and on (or close to) the sample surface.

Discussion

According to composition, the synthesized samples can be divided into two groups. The chalcopyrite group (samples 1–6) includes gold of high fineness (84–96 wt.%) and Ag-Au sulfides associated with tetragonal chalcopyrite, cubanite, talnakhite, pyrite, bornite, and pyrrhotite. The haycockite group (samples 7–9) includes gold of high fineness (80–82 wt.%) and silver (98–99 wt.%) associated with haycockite, bornite, and pyrrhotite. Gold of high fineness and products of the iss crystallization were identified in both groups. However, in the chalcopyrite assemblages, Ag-Au sulfides are formed simultaneous with gold, whereas silver crystallizes in the assemblages of haycockite, which is depleted in S in comparison with tetragonal chalcopyrite $CuFeS_2$. It appears from this that crystallization of impurity phases depends on the iss composition and occur during two stages. Gold of high fineness and silver are formed at the first stage. Ag-Au sulfides in the samples of the chalcopyrite group crystallized at the second stage replacing gold and silver of the first stage.

The first stage is characteristic of all samples. Gold and silver are more refractory phases than iss; their alloys crystallize at 1060–960°C. The following crystallization of iss (900–850°C, Yund & Kullerud, 1966) is accompanied with accumulation of most crystallized impurities in residual melt. This is indicated by gold and silver grains at the boundaries of grains of chalcopyrite and haycockite, in pores, and on the sample surface together with pyrite and bornite crystallized after iss at 738° and 568°C (Yund & Kullerud, 1966).

The samples of the chalcopyrite group are enriched in S in comparison with iss. After iss crystallization, they are characterized by phase assemblages iss + S and iss + py + S, which persist in the Cu-rich field of the Cu-Fe-S system at 600°C (Fig. 1). At 568°C, assemblage iss + S in sample 6 changes is replaced by assemblage iss + bn, whereas assemblage iss + py + S in sample 1, by iss + py + bn. It allows concluding that Ag-Au sulfides are formed by the reaction of gold and silver with gaseous sulfur after crystallization of iss but before bornite. This conclusion is supported by the composition and phase relations of synthesized samples. In the chalcopyrite-bearing samples, silver was not identified but fine disseminated Ag-bearing phases which are not in the samples with haycockite were found. In addition, grains of Ag-Au sulfides are close to gold grains of higher fineness (up to 96 wt.%) than in samples with haycockite (up to 82 wt.%). From this it follows that at the formation of Ag-Au sulfides, Au and Ag are redistributed between Au-Ag alloy of high fineness deposited at the first stage and crystallized Ag-Au sulfide ($alloy_1 + S_g \rightarrow alloy_2 +$ sulfide), whereas Ag as sulfides is extremely fine disseminated in the iss. Thus, Ag-Au sulfides are formed at temperature higher than 600°C and are resulted from free sulfur after crystallization of high-temperature cubic (fcc) chalcopyrite solid solution. It is consistent with experimental study of the Ag-Au-S system, where solid solutions of sulfides $(Ag,Au)S_2$ are melted at 838–680°C (Barton, 1980).

Crystallization of Ag sulfides in the samples of chalcopyrite group does not rule out

probable incorporation of Ag into iss and bornite. However, Ag is not detected in the haycockite and associated bornite. It allows concluding that Ag identified in Cu-Fe sulfides of chalcopyrite group occurs as sulfide and incorporate neither iss nor bornite.

Change of phase composition of the samples below 600°C (crystallization of bornite, pyrrhotite and iss exsolution) does not effect on Au and Ag phases in the studied crystallized products of the Cu-Fe-S melts as demonstrated by the identical species of impurities and phase relations within haycockite and chalcopyrite groups of samples.

Despite Au and Ag content in the synthesized samples is higher than bulk concentration of these elements in natural minerals, minimum size of synthesized grains of Au-Ag phases determined by microscope resolution are consistent with results of Au and Ag study in natural mineral assemblages. Au-Ag solid solutions with Ag up to 20 wt.% are the most stable and frequent in nature (Yushko-Zakharova *et al.*, 1986). According to the results obtained, Au-Ag solid solutions of such composition crystallize in all synthesized samples before precipitation of Ag-Au sulfides. In magmatic deposits of the Noril'sk district, proper minerals are the major carriers of Au and Ag (Sluzhenikin & Mokhov, 2002). Solid solutions of gold and silver are the most abundant ranging from gold of high fineness (100%) to nearly admixture-free native silver. In this case, native silver is characteristic of talnakhite and mooihoekite ores and chalcopyrite-pyrite and chalcopyrite-bornite ores contains Ag-Au sulfide in addition to Au-Ag solid solutions. Au-Ag alloys are frequently zoned (Ag content increases toward the grain margins) and patchy (the composition varies in 10–30 wt.%). Like synthesized Cu-Fe sulfides of chalcopyrite group, in chalcopyrite of the Talnakh pentlandite-chalcopyrite ore, vein-let- and irregular-shaped segregations in which Ag reaches 30 wt.% and more are observed in electron microscope.

The results obtained are important to determine Au and Ag phases in the initial magmatic assemblages of Cu-Fe sulfides. However, the study of stability of the Au-Ag synthesized phases and their chemical composition depending on mineral assemblage is required to interpret content of Au and Ag impurities in initial sulfide melt resulting in sulfide ore of the Noril'sk type, their partitioning between phases during melt crystallization and redistribution caused by post-magmatic process.

Conclusions

1. The partitioning of Au and Ag impurities (by 1 wt.%) between phases in the crystallized products of the Cu-Fe-S melts depending on mineralogy of assemblages of Cu-Fe sulfides is identified. Gold of high fineness (80–82 wt.%) and silver (98–99 wt.%) associated with haycockite $Cu_4Fe_5S_8$ cubic (pc) solid solution, bornite Cu_5FeS_4, and pyrrhotite $Fe_{1-x}S$. Gold of high fineness (84–96 wt.%) and Au-Ag sulfides of Me_2S or Me_3S_2 types, in which Me is Ag – up to 48 at.%, Au – up to 23 at.%, Cu – up to 18 at.%, Fe – up to 2 at.%, are associated with tetragonal chalcopyrite solid solution $Cu_{1-x}Fe_{1+x}S_2$, cubanite $CuFe_2S_3$, talnakhite $Cu_9Fe_8S_{16}$, pyrite FeS_2, bornite, and pyrrhotite.

2. Ag-Au sulfides are formed at temperature higher than 600°C and resulted from a presence of free sulfur after crystallization of high-temperature cubic (fcc) chalcopyrite solid solution.

3. The relationship between phases in joint products crystallized from Cu-Fe-S melt is determined by accumulation of Au-Ag phases in residual melt during crystallization of cubic (fcc) chalcopyrite solid solution and fine scattering of Ag at the formation of Ag-bearing sulfides.

Acknowledgements

We thank to S.F. Sluzhenikin and A.V. Mokhov for BSE images of synthesized phases.

This study was supported by the Russian Foundation for Basic Researches (project no. 08-05-233).

References

Barton M.D. The Ag-Au-S system // Econ. Geol. **1980**. 75. P. 303–316.

Cabri L.J. New Data on phase relations in the Cu-Fe-S system // Econ. Geol. **1973**. 68. P. 443–454.

Genkin A.D., Distler V.V., Gladyshev G.D., et al. Sulfide Cu-Ni ores of the Noril'sk deposits. Moscow: Nauka, **1981**. 234 pp. (In Russian.)

Kravchenko T.A., Nigmatulina E.N. Experimental study of fine-dispersed Au and Ag formation in the crystallized products of Cu-Fe sulfide melt // Bull. Earth Sciences. Russian Academy of Sciences. **2007**. No 1. http://www.scgis.ru/russian/cp1251/h-dgggms/1-2007/informbul-1-2007 (In Russian.)

Kravchenko T.A., Pavlyuchenko V.S., Sluzhenikin S.F., Mokhov A.V. Au and Ag behavior during crystallization from melt of phase assemblages of the Cu-Fe-S system with chalcopyrite and pyrrhotite // XV Russian Conference on Experimental Mineralogy. Syktyvkar. Abstr. **2005**. P. 57–59 (In Russian.)

Lavrent'ev Yu.G., Usova L.V. The RMA-89 program for a Camebax-Micro electron microprobe // J. Analyt. Chem. **1991**. 46(1). P. 67–75. (In Russian.)

Merwin H.E., Lombard R.H. The System Cu-Fe-S // Econ. Geol. **1937**. V. 32. P. 203–204.

Sluzhenikin S.F., Mokhov, A.V. Au and Ag in deposits of the Noril'sk destrict // Proc. All-Russia Symp. "Geology, genesis, and mining problems of complete deposits of precious metals". Moscow. **2002**. P. 326–330. (In Russian.)

Sugaki A., Shima H., Kitakaze A., Harada H. Isothermal phase relations in the Cu-Fe-S system under hydrothermal conditions at 350°C and 300°C // Econ. Geol. **1975**. 70. P. 806–823.

Tsujmura T., Kitakaze A. New phase relations in the Cu-Fe-S system at 800°C; constraint of fractional crystallization of sulfide liquid // N. Jb. Miner. Mh. **2004**. 10. P. 433–444.

Vaughan D.J., Craig J.R. Mineral Chemistry of Metal Sulfides. London: Cambridge University Press, **1978**.

Yund R. A., Kullerud G. Thermal stability of assemblages in the Cu-Fe-S system // Jour. Petrology. **1966**. V. 7. P. 454–488.

Yushko-Zakharova O.E., Ivanov V.V., Soboleva L.N. et al. Minerals of precious metals. Handbook. Moscow: Nedra, **1986**. 272 pp. (In Russian.)